Journal of Orthopaedic Translation 26 (2021) 171–180

Contents lists available at ScienceDirect

Journal of Orthopaedic Translation

journal homepage: www.journals.elsevier.com/journal-of-orthopaedic-translation

Original Article

Regulation of differentiation of annulus fibrosus-derived stem cells using heterogeneous electrospun fibrous scaffolds

Pinghui Zhou [a,b,☆], Genglei Chu [c,☆], Zhangqin Yuan [c,☆], Huan Wang [c], Weidong Zhang [c], Yingji Mao [b], Xuesong Zhu [c,*], Weiguo Chen [c,*], Huilin Yang [c], Bin Li [c,*]

[a] Department of Orthopedics, The First Affiliated Hospital of Bengbu Medical College, Bengbu, Anhui, China
[b] Anhui Province Key Laboratory of Tissue Transplantation, School of Life Sciences, Bengbu Medical College, Bengbu, Anhui, China
[c] Departments of Orthopaedic Surgery and Urology, The First Affiliated Hospital, Orthopedic Institute, Medical College, Soochow University, Suzhou, Jiangsu, China

ARTICLE INFO

Keywords:
Annulus fibrosus
Annulus fibrosus-derived stem cells
Cell differentiation
Degenerative disc disease
Fiber size

ABSTRACT

Background: Tissue engineering of the annulus fibrosus (AF) shows promise as a treatment for patients with degenerative disc disease (DDD). However, it remains challenging due to the intrinsic heterogeneity of AF tissue. Fabrication of scaffolds recapitulating the specific cellular, componential, and microstructural features of AF, therefore, is critical to successful AF tissue regeneration.

Methods: Poly-L-lactic acid (PLLA) fibrous scaffolds with various fiber diameters and orientation were prepared to mimic the microstructural characteristics of AF tissue using electrospinning technique. AF-derived stem cells (AFSCs) were cultured on the PLLA fibrous scaffolds for 7 days.

Results: The morphology of AFSCs significantly varied when cultured on the scaffolds with various fiber diameters and orientation. AFSCs were nearly round on scaffolds with small fibers. However, they became spindle-shaped on scaffolds with large fibers. Meanwhile, upregulated expression of collagen-I gene happened in cells cultured on scaffolds with large fibers, while enhanced expression of collagen-II and aggrecan genes was seen on scaffolds with small fibers. The production of related proteins also showed similar trends. Further, culturing AFSCs on a heterogeneous scaffold by overlaying membranes with different fiber sizes led to the formation of a hierarchical structure approximating native AF tissue.

Conclusion: Findings from this study demonstrate that fibrous scaffolds with different fiber sizes effectively promoted the differentiation of AFSCs into specific cells similar to the types of cells at various AF zones. It also provides a valuable reference for regulation of cell differentiation and fabrication of engineered tissues with complex hierarchical structures using the physical cues of scaffolds.

The translational potential of this article: Effective AF repair is an essential need for treating degenerative disc disease. Tissue engineering is a promising approach to achieving tissue regeneration and restoring normal functions of tissues. By mimicking the key structural features of native AF tissue, including fiber size and alignment, this study deciphered the effect of scaffold materials on the cell differentiation and extracellular matrix deposition, which provides a solid basis for designing new strategies toward more effective AF repair and regeneration.

Introduction

Degenerative disc disease (DDD) is the leading cause of low back pain, which seriously impacts the life quality of patients and may lead to disability in the active population [1,2]. Among the fundamental structural units of the intervertebral disc (IVD), annulus fibrosus (AF) is critical for confining the nucleus pulposus (NP) and maintaining intradiscal pressure, and the integrity of it is essential for the maintenance of the healthy structure and biological functions of IVD [3]. Unfortunately, AF, once damaged, does not spontaneously heal and continues to degenerate [4]. In fact, AF degeneration constitutes a major cause of DDD [1,5]. While current conservative or surgical treatments may relieve the symptomatic pain, they cannot restore the normal biomechanics and biophysical functions of AF and IVD [6]. Instead, regeneration of AF

* Corresponding author. Soochow University (South Campus), 708 Renmin Road, Rm 308 Bldg 1, Suzhou, Jiangsu, 215007, China.
E-mail addresses: zhuxs@suda.edu.cn (X. Zhu), 15312172967@163.com (W. Chen), binli@suda.edu.cn (B. Li).
☆ These authors equally contributed to this study.

https://doi.org/10.1016/j.jot.2020.02.003
Received 5 November 2019; Received in revised form 2 February 2020; Accepted 6 February 2020
Available online 3 March 2020

through tissue engineering technique may represent a promising alternative to ultimately curing the disease [7]. However, such an approach remains challenging due to the substantial complexity of native AF tissue.

AF is a typical heterogeneous tissue with gradient changes in cellular phenotype, biochemistry, microstructure, and biomechanics along the radial direction [8,9]. Anatomically, AF consists of 15–25 angle-plied concentric fibrous layers. In native AF tissue, the outer lamellae mainly contain fibroblast-like cells, which predominantly produce type I collagen, while the inner lamellae mainly contain chondrocyte-like cells, which produce type II collagen and proteoglycans. Collagen-I, collagen-II, and aggrecan, the major extracellular matrix (ECM) of AF tissue, have differential distribution in various AF regions [10,11]. As collagen-I mainly exists in the outer AF (oAF) region, yet collagen-II and aggrecan are mainly in the inner AF (iAF) region, they are considered as phenotypic markers of cells in these regions [12,13]. In addition, in iAF the fibers are less oriented, while those in oAF are highly aligned [9]. Such a hierarchical and well-organised structure of AF is essential to maintaining its biomechanical stability and physiological functions [5,10]. Previously, we have found that the thin type II collagen fibers (74 ± 7 nm) in iAF gradually change into thicker type I collagen fibers (182 ± 18 nm) in oAF and as a result, altered the biochemical and structural properties of matrix [14]. Therefore, effective replication of the region-specific feature of AF is critical for fabricating scaffolds for AF tissue engineering.

Another challenge of AF tissue engineering is the heterogeneous distribution of cell type. There are currently no specific surface markers to distinguish the phenotypes of cells from various AF regions. However, a number of studies have revealed that there are distinct cell types from the inner and outer regions of AF and of them, collagen-I, collagen-II, and aggrecan genes can be considered as specific marker genes, meaning that they can be used to distinguish iAF cells from oAF cells in human, rabbit, and bovine tail IVDs. For example, collagen-I can be considered as a phenotypic marker for oAF cells, while collagen-II and aggrecan as markers for iAF cells [7–14]. Therefore, ideal AF tissue engineering requires various types of cells at different regions within a scaffold in order to produce ECMs corresponding to those in native AF tissue, which certainly constitutes a major technical challenge. Constructing a heterogeneous scaffold containing region-specific regulatory cues that can direct the differentiation of a single stem cell source toward desired cell phenotypes, therefore, appeals to be a more effective approach.

Controlling the physical features, such as microstructure and mechanical properties of scaffolds has been widely used to regulate the differentiation of stem cells [15,16]. The micro-to-nanoscale topography, including porosity and fiber size of fibrous scaffolds, plays a critical role in controlling the adhesion, proliferation, and differentiation of stem cells. For example, when neural stem/progenitor cells (NSCs) were cultured on electrospun fibrous scaffolds with various fiber diameters, their proliferation and differentiation significantly depended on the fiber size [17,18]. When mesenchymal stem cells (MSCs) were seeded on chitosan fibrous scaffolds and sponges, it was found that chondrogenesis was superior on microfibers compared to macroporous sponges [19]. Similarly, the osteogenic differentiation of human periodontal ligament stem cells (hPLSCs) could be regulated by the micro-/nanostructure of the hydroxyapatite-coated porcine acellular dermal matrix [20]. Recently, we have also found that the fiber orientation and elasticity of electrospun scaffolds effectively affected the gene expression of annulus fibrosus-derived stem cells (AFSCs), a unique AF tissue-specific cell source that may differentiate into all types of resident cells in native AF tissue and showed great potential for AF repair and regeneration [21–23].

Therefore, in this study, we aimed to regulate the differentiation of AFSCs using the microstructural cues of a single material, which may ultimately lead to the fabrication of engineered AF with heterogeneous cellular, biochemical, and architectural characteristics as native AF tissue. To this end, we fabricated poly-l-lactic acid (PLLA) fibrous membranes with different fiber diameters using the electrospinning technique to mimic the different regions of AF. We found that different fiber sizes successfully regulated the differentiation of AFSCs into various cell types showing similar gene expression patterns as native AF tissue cells do. Further, assembly of different electrospun fibrous membranes with specifically differentiated AFSCs led to a piece of engineered AF tissue mimicking the hierarchical stratified structure of native AF tissue (Scheme 1).

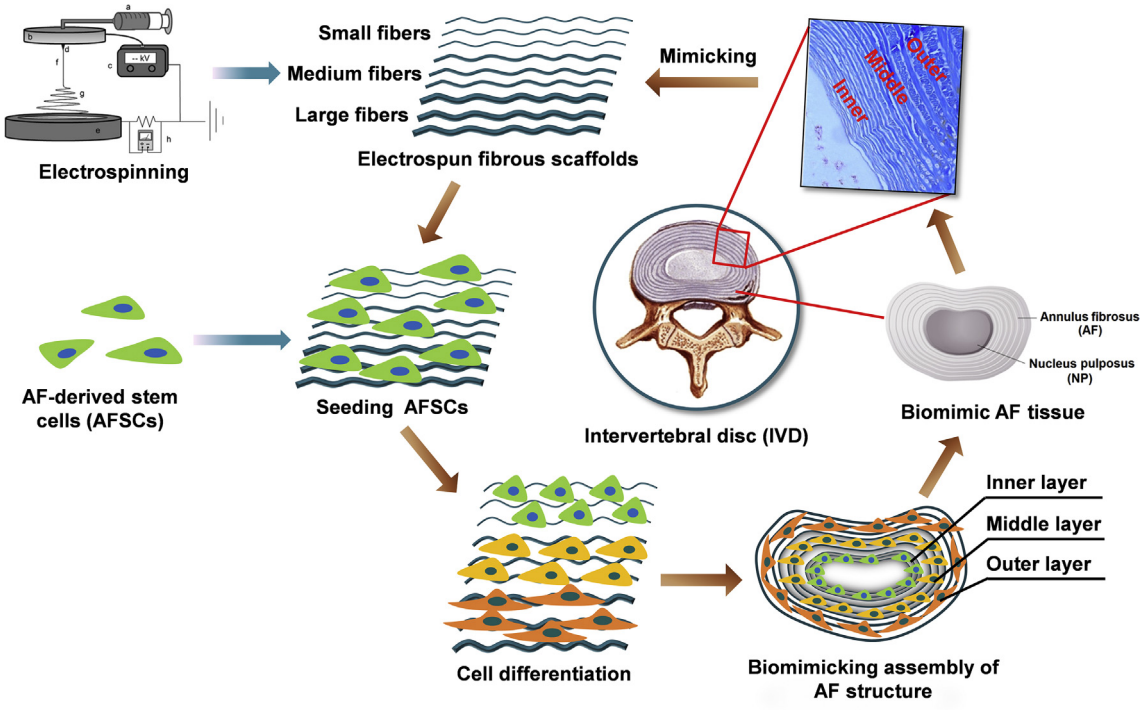

Scheme 1. Assembly of different electrospun fibrous membranes with specifically differentiated AFSCs led to a piece of engineered AF tissue mimicking the hierarchical stratified structure of native AF tissue.

Materials and methods

Fabrication of electrospun fibrous scaffolds with different diameters

Poly-L-lactic acid (PLLA) fibrous scaffolds with various fiber diameters were fabricated using the electrospinning technique by changing the concentration of PLLA in the feeding solution. In brief, PLLA was dissolved in a mixture of N, N-dimethylformamide, and dichloromethane (1:2 by weight) to prepare 11, 15, and 25 wt % PLLA solutions for fabricating small (**Small-F**), medium (**Medium-F**) and large (**Large-F**) fibers, respectively. The solution was loaded into a 5 ml plastic syringe with an 18G needle and fed at a constant rate of 200 μl/min using a syringe pump (Longer Pump Co., Ltd, China). A voltage of 15 kV was applied to the needle using a high-voltage power unit (Tianjin High Voltage Power Supply Co., Ltd, China). The distance between the syringe needle and the receiver was set at 15 cm. A rotating disk was used as the collector of the electrospun fibers. A rotating speed of 2000 rpm/min was used for collecting scaffolds with aligned fibers. The prepared scaffolds were dried in vacuum overnight before further experiments.

Characterisations of electrospun scaffolds

The morphology and microstructure of random and aligned PLLA scaffolds with different diameters were observed using a scanning electron microscopy (SEM, S-4800, Hitachi Co., Ltd., Japan). The average fiber diameter and pore size of the scaffolds were analyzed by Image J software. The wettability of the scaffolds was evaluated by measuring the water contact angles with sessile drop shape method and a drop shape analysis system at 25 °C. For measuring the mechanical properties of the scaffolds, the fibrous membranes were cut into 15.0 × 3.0 × 0.13 mm^3 specimens and evaluated through uniaxial tensile tests at a speed of 5 mm/min^{-} using a mechanical testing machine (Hengyi Co., Ltd., China).

Isolation and culture of rabbit AFSCs

AFSCs were isolated from AF tissue of New Zealand white rabbits (4–6 weeks old) and cultured in Alpha's modified Eagle's medium (Hyclone, SH30265.01B) with about 10% fetal bovine serum (FBS, SV30087.02; Hyclone) in accordance with the procedures in our previous study [9]. Briefly, we harvested the rabbit spinal columns from T10 to L5 under a sterile environment and removed the surrounding muscles and ligaments. Then the spinal column of each IVD was transversally sectioned. After carefully removing the NP, the pure AF tissue was minced and digested in Dulbecco's Modified Eagle Medium (low glucose) (DMEM-LG) medium (SH30021.01B; Hyclone, Thermo Fisher Scientific, Hudson, NH, USA) with Collagenase I (150 U/ml) and Collagenase II (150 U/ml) for 2–4 h. The obtained suspension was then centrifuged at 1000 rpm for 5 min, and then the cell pellet was re-suspended in DMEM-LG, including 15% FBS, 100 U/ml penicillin, 100 μg/ml streptomycin and maintained in the humidified incubator at 37 °C with 5% CO_2 at a density of 200–500 cells/ml.

Cell proliferation on the scaffolds

Before cell culturing, the electrospun PLLA membranes were cut into rounded samples fitting in a 96-well cell culture plate and then sterilised with Co-60 irradiation. Afterward, the AFSCs were seeded on the scaffolds at a density of 5 × 10^3 cells per well. The cells were cultured in a humidified incubator at 37 °C with 5% CO_2 for 1, 3, 5, 7 days. After culturing, the cells were washed with PBS, and then 20 μl MTS assay reagent (CellTiter 96 Aqueous, Promega) and 100 μl medium were added into each well. After 3 h of incubation, a microplate reader (BioTek Instruments) was used to measure the absorbance at 490 nm.

Cell morphology visualisation

Cytoskeleton staining and SEM were applied to observe the morphology of cells cultured on the random and aligned electrospun fibrous membrane with different fiber diameters. First passage AFSCs were cultured on different scaffolds in DMEM-LG supplemented with 10% -FBS and 1% penicillin/streptomycin for 3 days. For cytoskeleton staining, the cells were washed twice with PBS, fixed with 4% paraformaldehyde for 15 min, and permeabilised with 0.1% Triton X-100 for 5 min. The cells were then stained with fluorescein isothiocyanate (FITC)-phalloidin (Enzo Biochem, New York, NY, USA) and DAPI (Roche, Basel, Switzerland) for labelling F-actin and nuclei, respectively. After washing with PBS, the morphology of cells was recorded using a fluorescence microscope (Zeiss Axiovert 200, Carl Zeiss Inc, Thornwood, NY). For SEM observation, the cells on the scaffolds were rinsed twice with PBS after culturing. The cells were fixed using 2.5% glutaraldehyde for 2 h and then rinsed with deionised water for three times. The samples were dehydrated with graded ethanol from 10% to 100% for 15 min, and then were dried and sputter-coated with gold. The morphology of the cells was then observed using SEM at an accelerating voltage of 4 kV.

Real-time quantitative polymerase chain reaction (RT-qPCR) analysis

The random and aligned PLLA fibrous membranes were sterilised using 75% alcohol. The rabbit AFSCs were then seeded on the scaffolds (5 × 10^5 cells/well) and incubated in the humidified incubator at 37 °C with 5% CO_2 for 7 days. Afterward, the scaffolds were washed three times with PBS, and the AFSCs were digested with 0.25% trypsin. The total RNA from the treated AFSCs was extracted using a TRIZOL isolation system (Invitrogen, Thermo Fisher Scientific, Hudson, NH, USA) following the manufacturer's protocol. Reverse transcription was performed using a Revert-Aid First-Strand cDNA Synthesis Kit (Fermentas, K1622) and oligo(dT) primers on a reverse transcription PCR system (Eastwin Life Science, Beijing). RT-qPCR was performed on a Bio-Rad CFX96 Real-Time System using the SsoFast EvaGreen Supermix Kit (Bio-Rad). The relative expression level of genes was analyzed using the $2^{-\Delta\Delta Ct}$ method normalised to the housekeeping gene glyceraldehyde-3-phosphate dehydrogenase (GAPDH), which served as an internal control. Relative quantitative gene expression was calculated and converted to percent expression compared to unstimulated cells. The sequences of primers used in this study are listed in Table 1.

Biochemical assays

After culturing for 7 days, the supernatants of cells cultured on the scaffolds were collected. The contents of collagen-I and collagen-II were determined using enzyme-linked immunosorbent assay (ELISA) kits (R&D Systems, USA) following the manufacturer's protocol. The total glycosaminoglycan (GAG0 content was quantified with the 1, 9-dimethylmethylene blue (DMMB) dye-binding assay using a commercially available kit (Genmed Scientifics Inc., USA, GMS 19239.2). The DNA content was determined using DNA-binding fluorochrome dye Hoechst 33258. The matrix synthesis of cells was normalised to the corresponding DNA content.

Histological and immunohistochemical evaluations

The PLLA scaffolds with different fiber diameters were sterilised using ultraviolet exposure (30 min per side) and incubated with fibronectin solution to promote cell adhesion prior to cell culture. Following that, AFSCs were cultured on the scaffolds for 7 days. Then the constructs were washed three times with PBS and fixed with 4% phosphate-buffered paraformaldehyde for 30 min at 4 °C. The fixed cells on the scaffolds were dehydrated through a graded series of ethanol from 10% to 100%, overlaid the scaffolds of different diameters with cells embedded in paraffin, and then sectioned into 8 μm-thick slices. Then the slides were

Table 1
Sequences of primers for RT-qPCR.

Gene	Forward	Reverse	Accession number
GAPDH	5′-ACTTTGTGAAGCTCATTTCCTGGTA-3′	5′-GTGGTTTGAGGGCTCTTACTCCTT-3′	NM_001082253
Collagen-I	5′-CTGACTGGAAGAGCGGAGAGTAC-3′	5′-CCATGTCGCAGAAGACCTTGA-3′	AY633663
Collagen-II	5′-AGCCACCCTCGGACTCT-3′	5′-TTTCCTGCCTCTGCCTG-3′	NM_001195671
Aggrecan	5′-ATGGCTTCCACCAGTGCG-3′	5′-CGGATGCCGTAGGTTCTCA-3′	XM_002723376

treated using hematoxylin for 6 min and eosin for 1 min and were checked using a Zeiss Axiovert 200 inverted phase contrast microscope (Carl Zeiss Inc., Thornwood, NY).

Statistical analysis

All data are provided as the mean ± standard deviation (SD). The statistical analyses were performed by SPSS software. Kruskal–Wallis one-way analysis of variance (ANOVA) tests followed by Tukey post hoc tests were used. Unpaired student's *t*-tests were also used where appropriate. A difference between two groups is considered statistically significant if p is less than 0.05.

Results

Fabrication of fibrous scaffolds with various fiber diameters

The electrospinning technique was used to fabricate random and aligned fibrous PLLA scaffolds with different fiber diameters. Fibers with increased diameter were obtained by increasing the concentration of PLLA. On average, the diameters of the small, medium, and large random fibers were 0.55 ± 0.09 μm, 1.07 ± 0.18 μm, and 3.29 ± 0.53 μm, respectively, and those of aligned electrospun fibers are 0.50 ± 0.08 μm, 1.00 ± 0.16 μm, and 3.19 ± 0.19 μm, respectively (Fig. 1).

The water contact angles of scaffolds were similar among random and aligned scaffolds (about 135°) irrespective of the fiber diameter (Fig. 2A and B). The strength of scaffolds increased with a fiber diameter of scaffolds irrespective of the orientation of fibers. The tensile strength of random electrospun membranes with small, medium, and large diameters was 1.23 ± 0.32, 1.65 ± 0.22, and 1.82 ± 0.2 MPa, respectively, while that of aligned electrospun membranes was 1.19 ± 0.22, 1.48 ± 0.3, and 1.96 ± 0.3 MPa, respectively. The breaking elongations of random electrospun membranes with small, medium, and large diameters were measured to be 52.69 ± 0.66, 49.68 ± 0.61, and 28.49 ± 0.56%, respectively, and those of aligned electrospun membranes were 52.79 ± 0.52, 48.76 ± 0.72, and 27.73 ± 0.62%, respectively (Fig. 2C and D). However, the tensile moduli of all scaffolds were similar, and no significant difference was observed between random and aligned scaffolds.

Proliferation of AFSCs

MTS assays were performed to evaluate the proliferation of AFSCs cultured on the random and aligned fibrous scaffolds with different fiber diameters after 1, 3, 5, and 7 days (Fig. 3). AFSCs grown on standard tissue culture polystyrene (TCPS) dishes were used as a control group. AFSCs proliferated well on all random scaffolds independent of fiber diameter. Similar results were observed for cells on aligned fibrous scaffolds. Moreover, no obvious difference was observed on the number of AFSCs cultured on random and aligned scaffolds on the same day. However, AFSCs appeared to grow faster on all scaffolds than those on TCPS, likely as a result of the markedly larger aspect surface area of electrospun fibrous scaffolds. Therefore, AFSCs proliferated well on all the scaffolds irrespective of their microstructure, suggesting that all the scaffolds provided suitable environments for cell proliferation.

Morphology of AFSCs

The morphology of AFSCs was visualised by cytoskeleton staining using FITC-phalloidin. The cytoskeleton micrographs show that AFSCs attached well to all scaffolds irrespective of the microstructure, but they displayed distinct morphology on the scaffolds with various fiber diameters (Fig. 4). On the random fibrous scaffold with small fiber diameter, the morphology of AFSCs was relatively round, while elongated and spindle AFSCs were observed on the random fibrous scaffold with large fiber diameter. The same results were observed for AFSCs cultured on aligned fibrous scaffold with various fiber diameters. AFSCs aligned parallel to the fibers on aligned fibrous scaffolds, whereas the cells cultured on random fibrous scaffolds spread out and exhibited polygonal morphology. In general, AFSCs on aligned scaffolds were more elongated

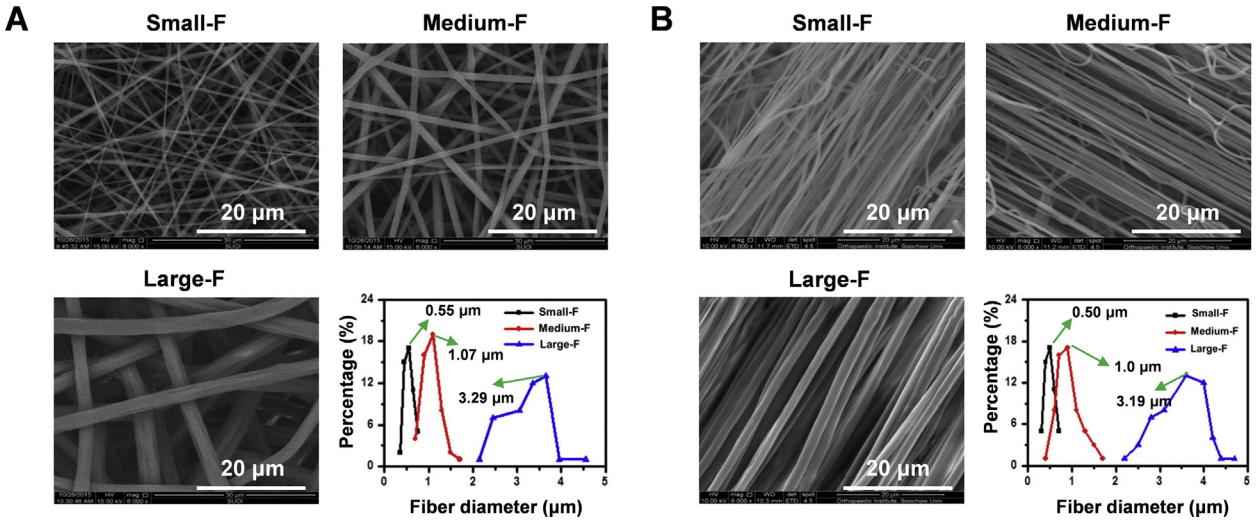

Figure 1. The microstructure of scaffolds observed using SEM. (A) Morphology of the random electrospun fibers with small, medium, and large diameters, varying from 0.55 μm to 3.29 μm; (B) morphology of the aligned electrospun fibers with small, medium, and large diameters, varying from 0.5 μm to 3.19 μm.

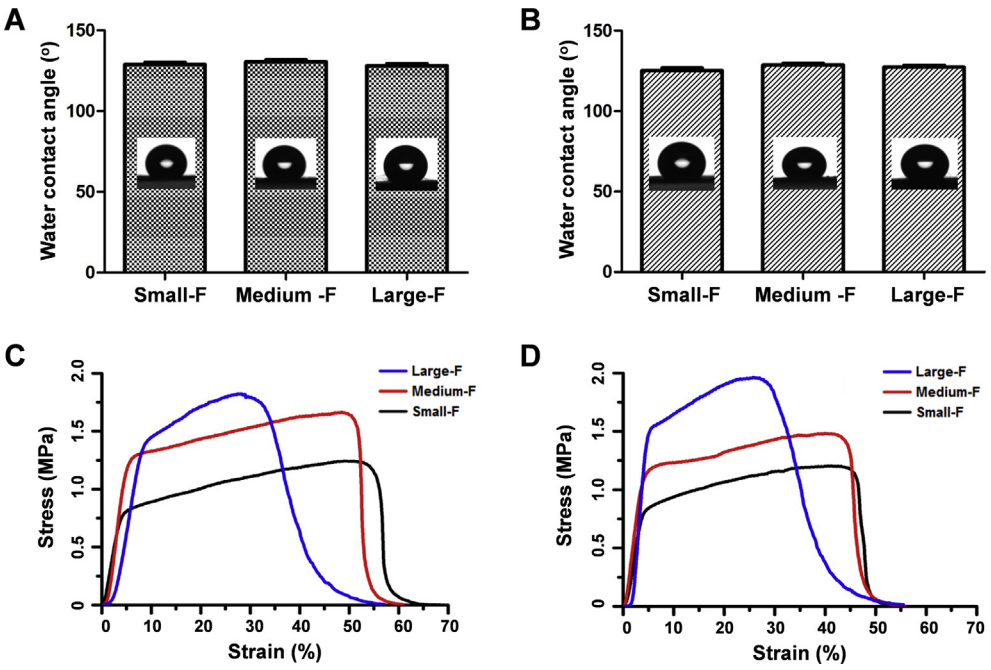

Figure 2. (A–B) Water contact angle and mechanical properties of the random (A) and aligned (B) electrospun fibrous scaffolds. (C–D) The stress–strain curves of the random (C) and aligned (D) fibrous scaffolds.

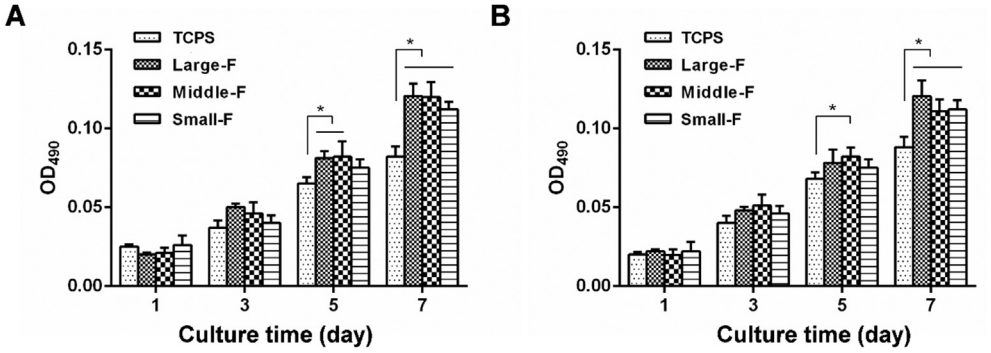

Figure 3. The proliferation of AFSCs on the fibrous scaffolds by MTS assays. (A) The proliferation of AFSCs on random scaffolds with various fiber diameters with TCPS as control. *, $p < 0.05$. (B) The proliferation of AFSCs on the aligned scaffolds with various fiber diameters with TCPS as control. *, $p < 0.05$.

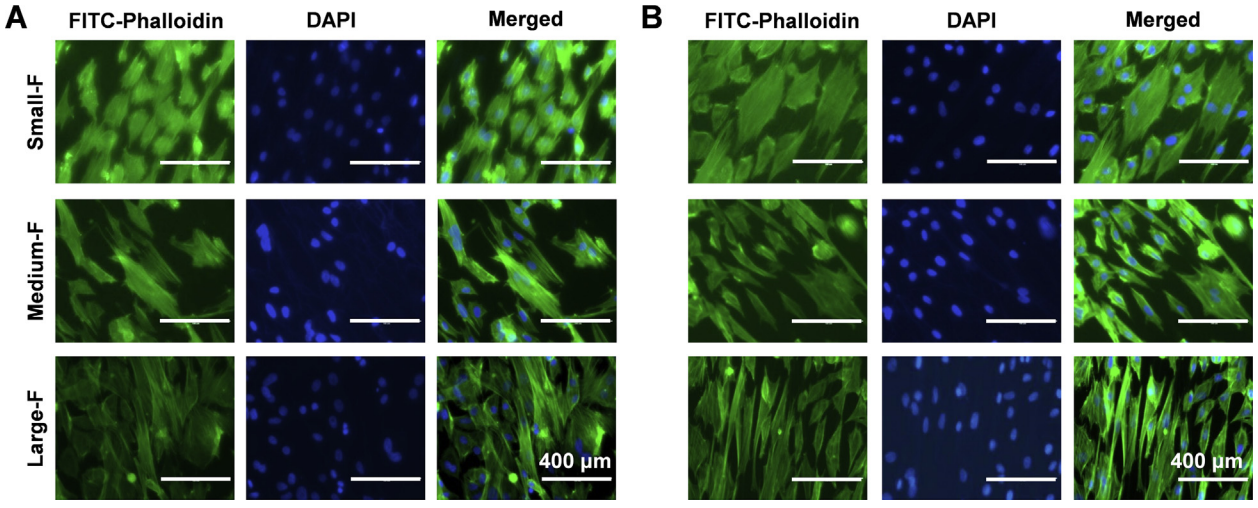

Figure 4. The morphology of AFSCs on the random (A) and aligned (B) fibrous scaffolds by cytoskeleton staining.

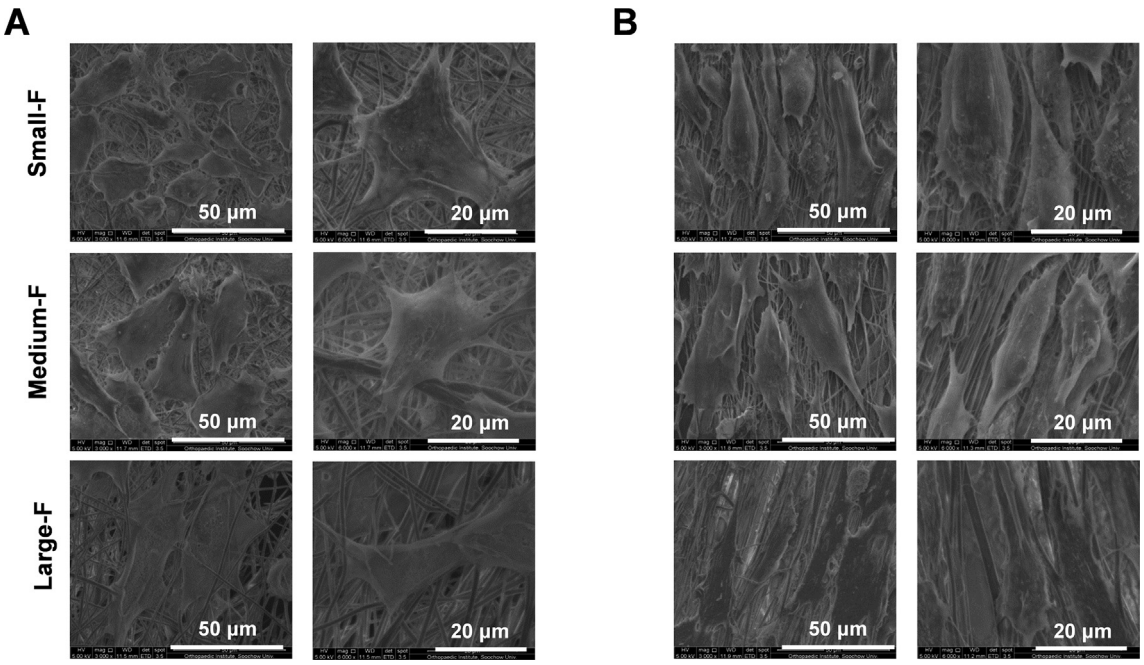

Figure 5. The morphology of AFSCs on the random (A) and aligned (B) fibrous scaffolds observed by SEM.

than those on random scaffolds with similar fiber diameter.

The morphology of AFSCs was further visualised by SEM (Fig. 5). The micrographs indicate that AFSCs attached well to all the fibrous scaffolds. Similar results were observed that AFSCs were relatively spread-out with a polygonal phenotype on random scaffolds with smaller fiber diameters, while they were spindle-shaped on those with larger fiber diameters. The morphology of AFSCs on aligned scaffolds was more spindle-shaped than that on random scaffold with similar diameter, and there were fewer antennas in cells on aligned scaffolds.

Gene expression of AFSCs

The gene expression of collagen-I, collagen-II, and aggrecan, which are the major matrix components of native AF tissue, were analyzed in AFSCs cultured on random and aligned fibrous PLLA scaffolds using RT-qPCR (Fig. 6). For both random and aligned scaffolds, the gene expression of collagen-I in AFSCs increased with fiber diameter after culturing for 7 days, while the opposite trend was observed for the gene expression of collagen-II and aggrecan. However, the gene expression of collagen-II and aggrecan showed no significant difference in the scaffolds with small and middle diameters. In addition, the gene expression of collagen-I and aggrecan in AFSCs cultured on aligned scaffolds was higher than those on random scaffolds with similar diameters, while the gene expression of collagen-II was similar for cells cultured on random and aligned scaffolds with similar diameters.

Biochemical contents of AFSCs

Further, the contents of major AF matrix components in AFSCs were determined using ELISA (Fig. 7). The content of collagen-I in AFSCs increased with fiber diameter on random fibrous scaffolds after 7 days of culture, being 2.97 ± 0.45, 7.80 ± 1.42, and 12.30 ± 1.80 ng/μg on scaffolds with small, medium, and large fibers, respectively. The content of collagen-II was 7.97 ± 0.45, 7.46 ± 0.95, and 4.63 ± 0.90 ng/μg, respectively, and that of GAG was 10.97 ± 0.45, 10.80 ± 0.74, and 6.63 ± 0.90 ng/μg, respectively, for AFSCs cultured on the above scaffolds. No obvious difference was observed for the content of collagen-II and GAG between the scaffolds with the small and medium diameter. Similar results were found for AFSCs cultured on aligned fibrous scaffolds, with the content of collagen-I being 7.31 ± 0.91, 9.46 ± 0.95, and 16.30 ± 1.80 ng/μg, the content of collagen-II being 9.46 ± 0.80, 8.32 ± 0.90, and 4.54 ± 0.70 ng/μg, and the content of GAG being 13.46 ± 0.80, 13.32 ± 0.90, and 8.54 ± 0.70 ng/μg, respectively, in the cells cultured on scaffolds with small, medium, and large fibers, respectively. On the other hand, the contents of collagen-I and GAG for the aligned scaffolds were higher than that for the random scaffolds with the same diameter, while the contents of collagen-II on the aligned scaffolds and random scaffolds showed no significant difference. These results were in accordance with the PCR analysis, confirming that the gene expression of AFSCs was influenced by the fiber size of the scaffolds.

Culture of AFSCs on a multi-layer construct

As a proof-of-concept test, a three-layer fibrous construct was prepared by overlaying scaffolds with various fiber sizes to mimic the structural characteristics of AF. After 7 days of culture of AFSCs on the construct, H&E staining of its sections showed that AFSCs were spindle-shaped in the region of large fibers, while they were almost round-shaped in the region of small fibers. The cells in the region with medium-sized fibers were between round and spindle-shaped (Fig. 8).

Discussion

During tissue development and regeneration, the microenvironment of matrix or biomaterial provides physical (e.g., structural and mechanical factors), chemical (e.g., functional groups and bioactive molecules), and biological (e.g., growth factors) cues that direct fundamental cell behaviors (including cell morphology, orientation, migration, and differentiation) toward tissue formation. While the development of biomaterials has traditionally been based on a new chemistry, there is growing recognition that the physical properties of materials can regulate biological responses. Numerous studies have shown that the structure and geometry of scaffolds, such as porosity, pore shape, and size, could significantly affect the behaviors of stem cells, and therefore, play an

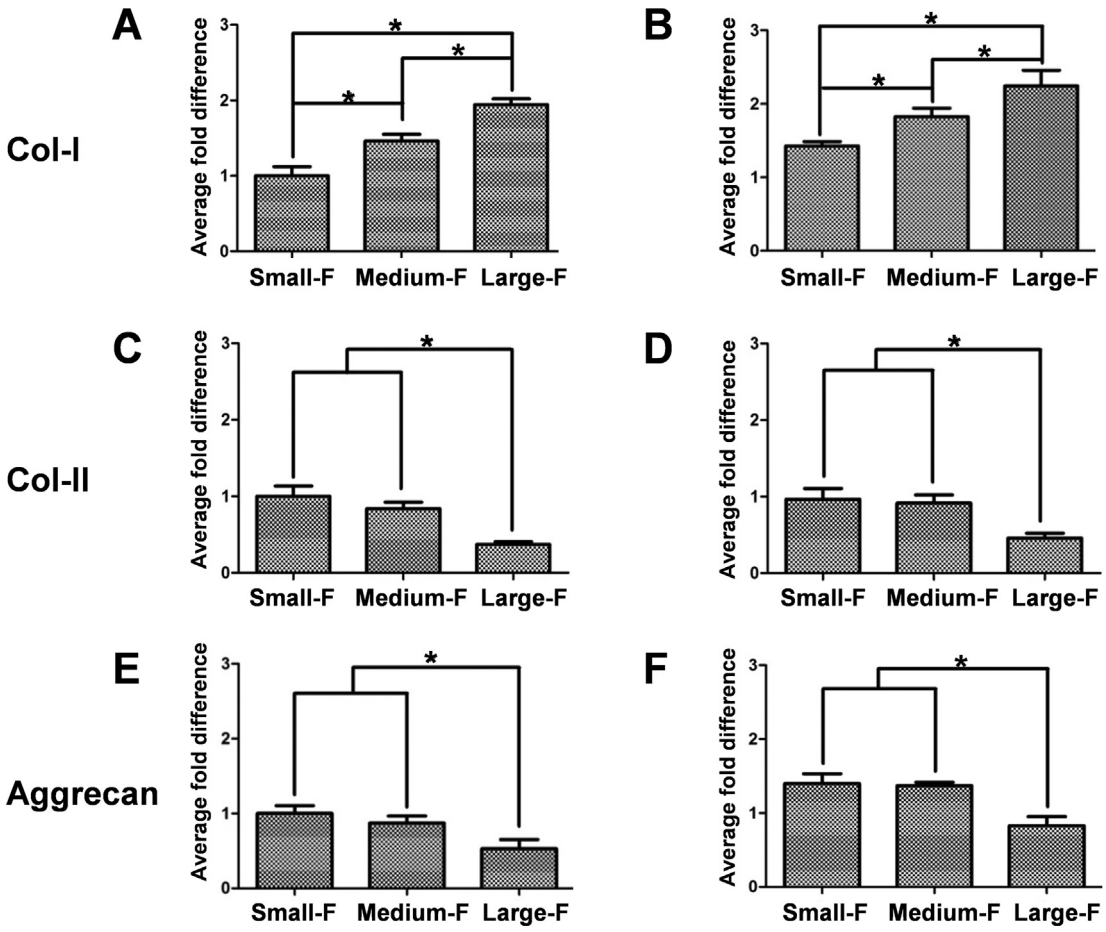

Figure 6. Gene expression of collagen-I, collagen-II, and aggrecan of AFSCs cultured on the random (A, C, and E) and aligned (B, D, and F) fibrous scaffolds determined using RT-qPCR. *, $p < 0.05$.

essential role in tissue regeneration [17,24]. For example, Di Luca et al. prepared constructs with a discrete gradient in pore size to mimic the architecture of long bone tissue, which is characterised by a structural gradient. Culturing of human mesenchymal stromal cells (hMSCs) on them revealed a correlation between osteogenic differentiation and ECM mineralisation and pore dimension [25]. Micropatterned islands of varying diameters have also been used to modulate the differentiation efficiency of endothelial cells (ECs) [26].

AF is a complex heterogeneous tissue with hierarchical microstructures and gradient changes along the radial axis. One of the major barriers to successful AF regeneration is to simultaneously regenerate different regions of AF tissue with appropriate biochemical, biomechanical, and microstructural characteristics, which play a pivotal role in maintaining normal biological and mechanical functions of native AF tissue. To date, there have been many attempts to fabricate scaffolds mimicking the microstructure and mechanical features of AF using natural or synthetic biomaterials [27]. Bhattacharjee et al. fabricated aligned electrospun fibrous silk membranes to mimic the anatomical fibrous orientation features of AF [10]. In our previous study, we fabricated electrospun polyurethane (PU) scaffolds with different elasticity for AFSC culture. We found that AFSCs, upon culturing on stiff, medium, and soft scaffolds, were able to differentiate into the types of cells close to those at the outer, middle, and inner regions of AF, respectively [22,23]. Nevertheless, such scaffolds only partially mimicked the mechanical property and orientation features of AF, but could not replicate the complex hierarchical structure of AF. In this study, we took advantage of the electrospinning technology to fabricate fibrous scaffolds with small, medium, and large fiber diameters using a single material to mimic the microstructural features of the inner, middle, and outer regions of native AF tissue. Building on this, we tried to study the differentiation of AFSCs in response to the fiber size of scaffolds.

Cells can sense and generate internal forces for measuring the microenvironment. When cultured on scaffolds with increasing geometric stiffness, cells sense the matrix through integrin-mediated focal adhesions (FAs), and increasing traction forces are generated by actin polymerisation and myosin II-dependent contractility to deform the substrate [28]. In our previous study, we examined the effect of cell shape on collagen-I expression in human tendon fibroblasts and found that elongated cells expressed more collagen-I than less elongated cells, likely as a result of altered cytoskeletal tension-induced mechanotransduction [29]. In addition, our results show a significant contact guidance effect in that fiber orientation strongly regulated the alignment and shape of AFSCs on the fibrous scaffolds. It should be mentioned that the orientation of AFSCs might be more critical for the formation of AF lamella. The morphology of AFSCs on the scaffolds with large fiber diameter was spindle-like, while it was relatively round on the small-fiber-diameter scaffolds, irrespective of the alignment of fibers (Figs. 4 and 5). The enhanced cell spreading might account for this, which increased their cytoskeletal tension and deformation to activate Wnt, Yes-associated protein (YAP), and c-Jun N-terminal kinase (JNK) signalling pathways and lead to changes in gene expression. This suggests that controllable geometrical parameters, such as fiber size and fiber orientation, might affect cell functions, such as differentiation [30]. These results suggest that the microstructure of scaffolds effectively affected the morphology of cells with phenotypes resembling the types of cells in the outer, middle, and inner regions of native AF tissue.

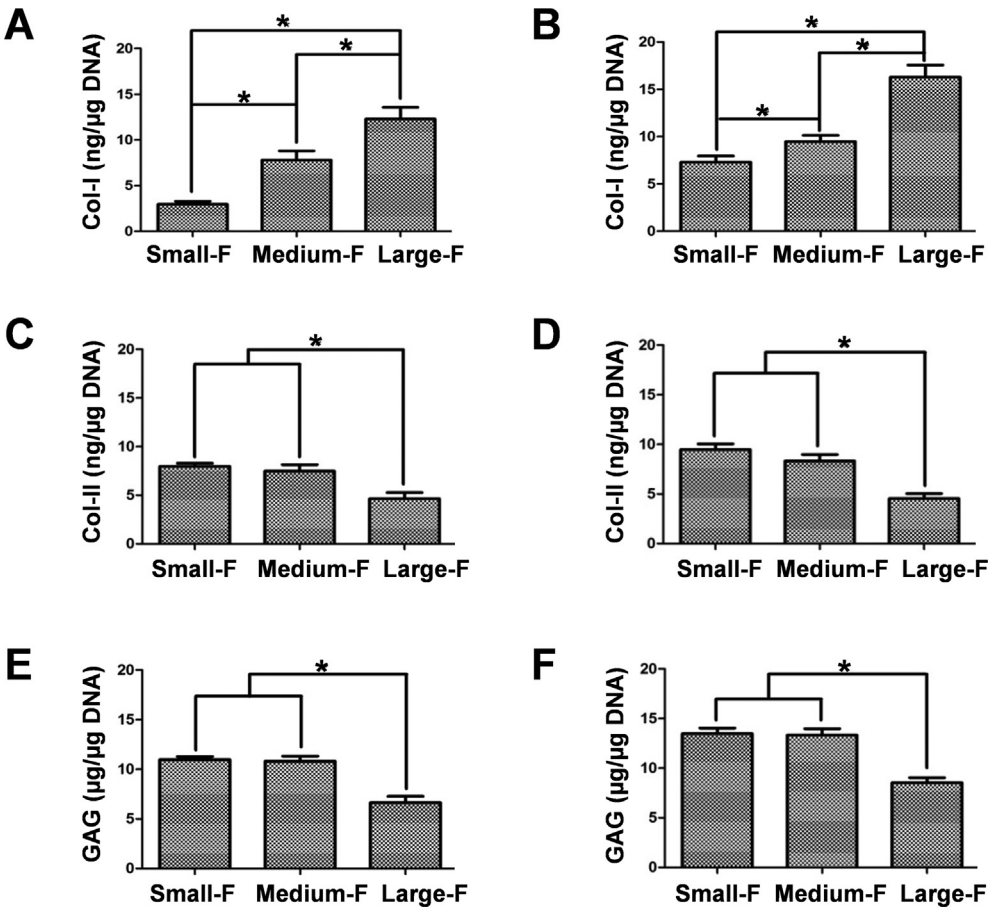

Figure 7. Protein contents of collagen-I, collagen-II, and aggrecan of AFSCs on the random (A, C, and E) and aligned (B, D, and F) fibrous scaffolds measured using ELISA. *, $p < 0.05$.

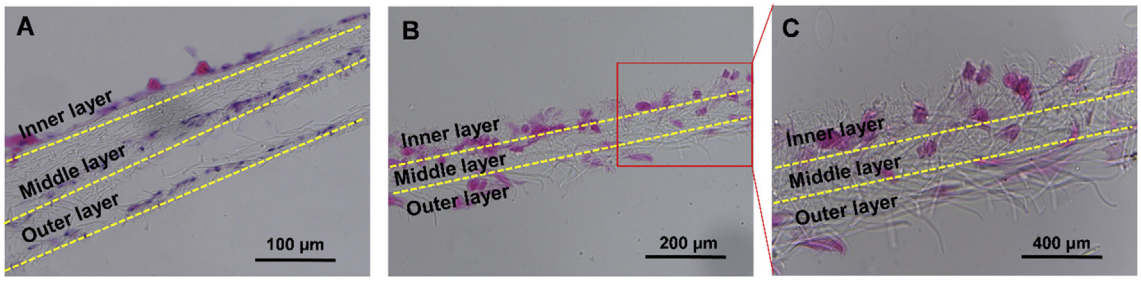

Figure 8. H&E staining of AFSCs on overlaid fibrous scaffolds with various fiber diameters.

Since AF is a fibrocartilage tissue, collagen-I, collagen-II, aggrecan are considered characteristic matrix molecules of AF tissue. Nakamichi et al. demonstrated that the expression of newly synthesised ECM (collagen-I, collagen-II, and aggrecan) of AF was in relation to the regulation of multiple tendon/ligament-related genes [31]. We found that the gene expression and protein production of collagen-I in AFSCs on the scaffold with small fiber diameter was relatively low, whereas the gene expression of collagen-II and aggrecan was relatively high. On the other hand, the gene expression and protein production of collagen-II and aggrecan showed an opposite behavior when AFSCs were cultured on scaffolds with large fiber diameter (Fig. 6). It is known that in native AF tissue, the phenotype of AF cells gradually changes from fibroblast-like in the outer zone to chondrocyte-like in the inner zone. Correspondingly, the contents of collagen-II and aggrecan decrease from the inner to the outer zone of AF, while the content of collagen-I increases. Therefore, our results demonstrate that the differentiation of AFSCs was successfully regulated toward the specific types of cells residing in different regions of AF by controlling the fiber size of the scaffold. We also found that the gene expression and protein production of collagen-I and aggrecan in AFSCs on aligned scaffolds were higher than those on random scaffolds. However, the gene expression and protein production of collagen-II showed no apparent difference in these two types of scaffolds, implying that collagen-II expression might be insensitive to scaffold topography. This is in agreement with a previous study from Tobias et al., in which the fiber orientation of electrospun scaffolds did not result in a major difference in the collagen-II deposition of articular chondrocytes [32].

Cells reside in a 3D environment. It has been increasingly appreciated that cellular phenotypes are significantly affected by the reduction of dimensionality in which the mechanical and biochemical cues are presented to the cells. The phenotype of stem cells can greatly vary in a 3D environment compared to 2D culture systems. However, the current microstructure of the material is just limited to the 2D structure, which

induces the differentiation of stem cells into one type cell [33]. In our proof-of-concept study, AFSCs were cultured on a multilayered construct consisting of lamellar sheets that mimicked the microstructure of AF. H&E staining of the overlaid scaffolds with specifically differentiated AFSCs showed similar hierarchical structures to native AF tissue (Fig. 8). These results suggest that ideally, engineered AF tissue scaffolds should have microstructure variations along the radical direction to regulate the differentiation of stem cells into region-specific AF cells, which then secrete corresponding ECM to facilitate AF regeneration. However, a culture time as short as 7 days is indeed insufficient to generate the engineered tissues that mimic the native AF structures. Future studies will evaluate long-term implantation of engineered IVD constructs in vivo.

It is worth noting that irrespective of the fiber size of scaffolds, the production of matrices, including collagen-I, collagen-II, and aggrecan in AFSCs, was significantly lower than their levels in native AF tissue [34]. On the one hand, this certainly is a result of the markedly shorter time of cell culture (1–2 weeks) compared to tissue development (a few years). On the other hand, it may also imply that a mere single-factor regulation is not enough to drive the differentiation and maturation of stem cells toward specific tissue formation. Instead, the synergistic effects from a combination of factors, which better mimic the in vivo microenvironment, are desirable for achieving ideal tissue regeneration [17]. This echoes the opinion that when applied together with desired biochemical signals, topographical cues may more effectively regulate the lineage commitment of stem cells.

Conclusion

In summary, we have successfully fabricated electrospun fibrous scaffolds with various fiber sizes to mimic the microstructural characteristics of native AF tissue. The morphology of AFSCs on scaffolds with large fibers was spindle-shaped, while those on scaffolds with small fibers were relatively round. The gene expression and protein production of collagen-I in AFSCs increased with the fiber diameter of scaffolds, whereas those of collagen-II, aggrecan showed an opposite trend. Importantly, the changes in cell morphology, ECM gene expression, and protein production in response to fiber size were similar to those in different regions of native AF tissue. Together, these results provide a solid basis for AF regeneration by demonstrating the feasibility of regulating the differentiation of AFSCs through the fiber size of the scaffold.

Conflict of Interest

The authors have no conflicts of interest to disclose in relation to this article.

Acknowledgements

This work was supported by the National Key R&D Program of China (2016YFC1100203), National Natural Science Foundation of China (31530024, 81672213, 81702200, 31700854, 81925027), Scientific Research Foundation of Bengbu Medical College (BYKY1848ZD), Jiangsu Provincial Special Program of Medical Science (BL2012004), Jiangsu Provincial Clinical Orthopedic Center, Key Laboratory of Stem Cells and Biomedical Materials of Jiangsu Province and Chinese Ministry of Science and Technology, and the Priority Academic Program Development (PAPD) of Jiangsu Higher Education Institutions.

References

[1] Zeng Y, Chen C, Liu W, Fu Q, Han Z, Li Y, et al. Injectable microcryogels reinforced alginate encapsulation of mesenchymal stromal cells for leak-proof delivery and alleviation of canine disc degeneration. Biomaterials 2015;59:53–65.
[2] Li B, Chen D. Degenerative musculoskeletal diseases: pathology and treatments. J Orthop Transl 2019;17:1–2.
[3] Vergroesen PP, Kingma I, Emanuel KS, Hoogendoorn RJ, Welting TJ, van Royen BJ, et al. Mechanics and biology in intervertebral disc degeneration: a vicious circle. Osteoarthr Cartil 2015;23(7):1057–70.
[4] Chik TK, Ma XY, Choy TH, Li YY, Diao HJ, Teng WK, et al. Photochemically crosslinked collagen annulus plug: a potential solution solving the leakage problem of cell-based therapies for disc degeneration. Acta Biomater 2013;9(9):8128–39.
[5] Nerurkar NL, Baker BM, Sen S, Wible EE, Elliott DM, Mauck RL. Nanofibrous biologic laminates replicate the form and function of the annulus fibrosus. Nat Mater 2009;8(12):986–92.
[6] Martin JT, Milby AH, Chiaro JA, Kim DH, Hebela NM, Smith LJ, et al. Translation of an engineered nanofibrous disc-like angle-ply structure for intervertebral disc replacement in a small animal model. Acta Biomater 2014;10(6):2473–81.
[7] Lu J, Santerre JP, Kandel RA. Inner and outer annulus fibrosus cells exhibit differentiated phenotypes and yield changes in extracellular matrix protein composition in vitro on a polycarbonate urethane scaffold. Tissue Eng A 2014;20(23–24):3261–9.
[8] Bruehlmann SB, Rattner JB, Matyas JR, Duncan NA. Regional variations in the cellular matrix of the annulus fibrosus of the intervertebral disc. J Anat 2002;201(2):159–71.
[9] Li J, Liu C, Guo Q, Yang H, Li B. Regional variations in the cellular, biochemical, and biomechanical characteristics of rabbit annulus fibrosus. PloS One 2014;9(3):e91799.
[10] Bhattacharjee M, Miot S, Gorecka A, Singha K, Loparic M, Dickinson S, et al. Oriented lamellar silk fibrous scaffolds to drive cartilage matrix orientation: towards annulus fibrosus tissue engineering. Acta Biomater 2012;8(9):3313–25.
[11] Bhunia BK, Kaplan DL, Mandal BB. Silk-based multilayered angle-ply annulus fibrosus construct to recapitulate form and function of the intervertebral disc. Proc Natl Acad Sci U S A 2018;115(3):477–82.
[12] van den Akker GG, Surtel DA, Cremers A, Richardson SM, Hoyland JA, van Rhijn LW, et al. Novel immortal cell lines support cellular heterogeneity in the human annulus fibrosus. PloS One 2016;11(1):e0144497.
[13] van den Akker GGH, Koenders MI, van de Loo FAJ, van Lent P, Blaney Davidson E, van der Kraan PM. Transcriptional profiling distinguishes inner and outer annulus fibrosus from nucleus pulposus in the bovine intervertebral disc. Eur Spine J 2017;26(8):2053–62.
[14] Chu GL, Yuan ZQ, Zhu CH, Zhou PH, Wang H, Zhang WD, et al. Substrate stiffness- and topography-dependent differentiation of annulus fibrosus-derived stem cells is regulated by Yes-associated protein. Acta Biomater 2019;92:254–64.
[15] Abagnale G, Steger M, Nguyen VH, Hersch N, Sechi A, Joussen S, et al. Surface topography enhances differentiation of mesenchymal stem cells towards osteogenic and adipogenic lineages. Biomaterials 2015;61:316–26.
[16] Deng C, Chang J, Wu C. Bioactive scaffolds for osteochondral regeneration. J Orthop Transl 2019;17:15–25.
[17] Christopherson GT, Song H, Mao HQ. The influence of fiber diameter of electrospun substrates on neural stem cell differentiation and proliferation. Biomaterials 2009;30(4):556–64.
[18] Czeisler C, Short A, Nelson T, Gygli P, Ortiz C, Catacutan FP, et al. Surface topography during neural stem cell differentiation regulates cell migration and cell morphology. J Comp Neurol 2016;524(17):3485–502.
[19] Ragetly GR, Griffon DJ, Lee HB, Fredericks LP, Gordon-Evans W, Chung YS. Effect of chitosan scaffold microstructure on mesenchymal stem cell chondrogenesis. Acta Biomater 2010;6(4):1430–6.
[20] Ge S, Zhao N, Wang L, Liu H, Yang P. Effects of hydroxyapatite nanostructure on channel surface of porcine acellular dermal matrix scaffold on cell viability and osteogenic differentiation of human periodontal ligament stem cells. Int J Nanomed 2013;8:1887–95.
[21] Guo Q, Liu C, Li J, Zhu C, Yang H, Li B. Gene expression modulation in TGF-beta3-mediated rabbit bone marrow stem cells using electrospun scaffolds of various stiffness. J Cell Mol Med 2015;19(7):1582–92.
[22] Liu C, Zhu C, Li J, Zhou P, Chen M, Yang H, et al. The effect of the fibre orientation of electrospun scaffolds on the matrix production of rabbit annulus fibrosus-derived stem cells. Bone Res 2015;3:15012.
[23] Zhu C, Li J, Liu C, Zhou P, Yang H, Li B. Modulation of the gene expression of annulus fibrosus-derived stem cells using poly(ether carbonate urethane)urea scaffolds of tunable elasticity. Acta Biomater 2016;29:228–38.
[24] Moroni L, Licht R, de Boer J, de Wijn JR, van Blitterswijk CA. Fiber diameter and texture of electrospun PEOT/PBT scaffolds influence human mesenchymal stem cell proliferation and morphology, and the release of incorporated compounds. Biomaterials 2006;27(28):4911–22.
[25] Di Luca A, Ostrowska B, Lorenzo-Moldero I, Lepedda A, Swieszkowski W, Van Blitterswijk C, et al. Gradients in pore size enhance the osteogenic differentiation of human mesenchymal stromal cells in three-dimensional scaffolds. Sci Rep 2016;6:22898.
[26] Kusuma S, Smith Q, Facklam A, Gerecht S. Micropattern size-dependent endothelial differentiation from a human induced pluripotent stem cell line. J Tissue Eng Regen M 2017;11(3):855–61.
[27] Wan Y, Feng G, Shen FH, Laurencin CT, Li X. Biphasic scaffold for annulus fibrosus tissue regeneration. Biomaterials 2008;29(6):643–52.
[28] Piroli ME, Jabbarzadeh E. Matrix stiffness modulates mesenchymal stem cell sensitivity to geometric asymmetry signals. Ann Biomed Eng 2018;46(6):888–98.
[29] Li F, Li B, Wang QM, Wang JH. Cell shape regulates collagen type I expression in human tendon fibroblasts. Cell Motil Cytoskeleton 2008;65(4):332–41.

[30] Carbone A, Valente M, Annacontini L, Castellani S, Di Gioia S, Parisi D, et al. Adipose-derived mesenchymal stromal (stem) cells differentiate to osteoblast and chondroblast lineages upon incubation with conditioned media from dental pulp stem cell-derived osteoblasts and auricle cartilage chondrocytes. J Biol Regul Homeost Agents 2016;30(1):111–22.
[31] Nakamichi R, Ito Y, Inui M, Onizuka N, Kayama T, Kataoka K, et al. Mohawk promotes the maintenance and regeneration of the outer annulus fibrosus of intervertebral discs. Nat Commun 2016;7:12503.
[32] Schneider T, Kohl B, Sauter T, Kratz K, Lendlein A, Ertel W, et al. Influence of fiber orientation in electrospun polymer scaffolds on viability, adhesion and differentiation of articular chondrocytes. Clin Hemorheol Microcirc 2012;52(2–4):325–36.
[33] Yu W, Li R, Long J, Chen P, Hou A, Li L, et al. Use of a three-dimensional printed polylactide-coglycolide/tricalcium phosphate composite scaffold incorporating magnesium powder to enhance bone defect repair in rabbits. J Orthop Transl 2019;16:62–70.
[34] Blumenthal NR, Hermanson O, Heimrich B, Shastri VP. Stochastic nanoroughness modulates neuron-astrocyte interactions and function via mechanosensing cation channels. Proc Natl Acad Sci U S A 2014;111(45):16124–9.